A Novel Reconfiguration Strategy of a Delta-type Parallel Manipulator

Regular Paper

Albert Lester Balmaceda-Santamaría[1]*, Eduardo Castillo-Castaneda[1] and Jaime Gallardo-Alvarado[2]

1 Instituto Politecnico Nacional, CICATA Queretaro, Queretaro, QRO, Mexico
2 Department of Mechanical Engineering, Instituto Tecnologico de Celaya, Celaya, GTO, Mexico
*Corresponding author(s) E-mail: albert.balmaceda@gmail.com

Abstract

This work introduces a novel reconfiguration strategy for a Delta-type parallel robot. The robot at hand, whose patent is pending, is equipped with an intermediate mechanism that allows for modifying the operational Cartesian workspace. Furthermore, singularities of the robot may be ameliorated owing to the inherent kinematic redundancy introduced by four actuable kinematic joints. The velocity and acceleration analyses of the parallel manipulator are carried out by resorting to reciprocal-screw theory. Finally, the manipulability of the new robot is investigated based on the computation of the condition number associated with the active Jacobian matrix, a well-known procedure. The results obtained show improved performance of the robot introduced when compared with results generated for another Delta-type robot.

Keywords Reconfiguration, Kinematics Parallel Robot, Workspace, Screw Theory, Condition Number

1. Introduction

Nowadays, flexible manufacturing systems are highly advisable in order to increase, among other issues, the productivity and competitiveness of small and medium-sized manufacturing industries. In this context, a reconfigurable mechanism may be implemented owing to the fact that its topology can be quickly adjusted according to a specific task.

Industrial parallel robots, such as the well-known Delta robot, are currently used in electronic, food and pharmaceutical industries to perform pick-and-place tasks and many other tasks that require translational high-speed motions. A reconfigurable parallel robot can accomplish such industrial tasks more efficiently than a Delta robot, since these mechanisms have high levels of flexibility and the performance required to carry out complex assembly tasks.

In robotics, the reconfiguration concept is presented in [1] as the capacity to change the characteristics of robots when completing arbitrary operations. The main approaches that have been proposed for the reconfiguration of parallel mechanisms, such as the Stewart-Gough platform, are modular and variable geometric designs [2, 3, 29].

A modular manipulator consists of a set of modules that can be assembled into robots with different attributes. Modularity has been used recursively in parallel manipulators; see for example [4 - 14].

The reconfiguration of parallel manipulators using variable geometry consists of changing some dimensions of the robot with the purpose of generating new postures on the same parallel manipulator. In this context, the following should be cited: a double planar parallel reconfigurable manipulator presented in [15], the reconfigurable platform based on the Stewart-Gough platform [16], the reconfigurable parallel mechanism with an adjustable base designed in [17] and a new family of reconfigurable parallel mechanisms [18]. Furthermore, many authors (including some of the aforementioned) have used the redundancy sometimes generated by reconfiguration of the parallel manipulators for improving characteristics such as stiffness [19, 20, 21], force [22, 23], accuracy [24], increased workspace and singularity-free workspace [25 - 27], payload-capacity [28, 29], as well as performance indices like manipulability, condition number, global condition, dexterity and global dexterity [30 - 33].

Although reconfigurable parallel manipulators are a well-documented issue, some aspects thereof deserve in-depth investigated, primarily problems related to structural spaces. On the other hand, it is worth noting that the aforementioned mechanisms have a high level of mechanical complexity and therefore, the construction of physical prototypes can be an expensive option. In this regard, computer simulations generated with virtual prototypes is a cheaper and more viable alternative.

In this paper, a new reconfiguration of a 3-DOF Delta-type parallel robot, based on the concept of variable geometry, is presented. The reconfiguration is applied to a robot named Parallix LKF-2040, which was designed as a didactic version of a Delta-type parallel manipulator at the National Polytechnic Institute (IPN) in CICATA, Queretaro, Mexico [34]. The reconfiguration strategy proposed here is highly versatile, extremely simple and capable of returning to the original configuration and mechanical characteristics of the Parallix LKF-2040. Furthermore, the redundancy generated by the new manipulator allows for improving its kinematic performance, based on the computation of a performance index according to prescribed trajectories.

The paper is organized as follows: In section 2, the current mechanism and the proposed new reconfigurable system is described. The kinematic analysis is presented in section 3. In order to exemplify application of the method, in section 4, a case study is provided. Finally, conclusions are given in section 5.

2. Description of the Proposed Parallel Manipulator

Referring to Fig. 1, the Parallix LKF-2040, used as a base for creating the reconfiguration strategy, is a translational Delta-type parallel robot developed at IPN-CICATA. This manipulator is widely used for teaching purposes, owing to its convenient open architecture [34]. The Parallix comprises three stationary motors disposed angularly on its base through brackets. The motor axes are coupled to a

kinematic chain at the bracket level. Although the proposed mechanism closely resembles the famous Delta robot, it is in reality a 3-RUU robot, where R and U represent, respectively, for revolute and universal joints.
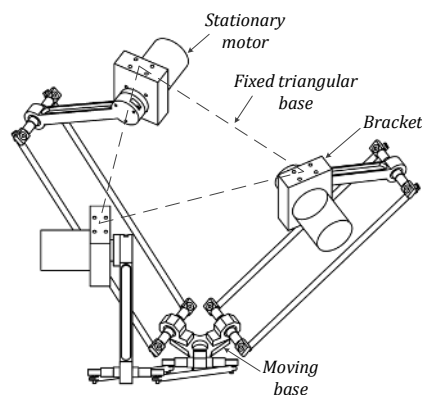

Figure 1. The Parallix LKF-2040 parallel manipulator

2.1 Reconfiguration proposal

As demonstrated by [35], the geometry of the fixed platform is the primary variable that significantly influences the workspace of the Parallix robot. Hence, in order to create an improved robot, the following requirements were considered for implementing a reconfiguration strategy of the Parallix robot: it must be mechanically simple, without adding weight and/or actuators to the kinematic chains, be able to change the entire workspace without modifying the lengths of links, increasing versatility without coupling or uncoupling links from the mechanism and minimize the structural space occupied by the robot. In Fig. 2, the conceptual design of the reconfigurable robot meeting such conditions is shown.
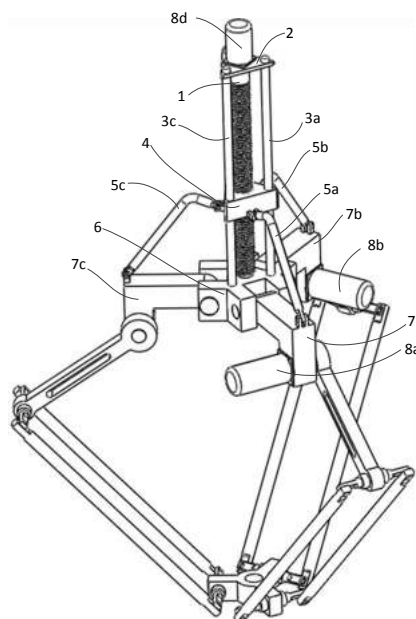

Figure 2. Proposed reconfiguration strategy. Patenting in process at the IMPI - Mexico: MX2013006781 (A).

The concept of this proposal is a redundant Delta-type parallel robot consisting of a reconfigurable fixed platform comprising a fixed element and mobile elements, which reconfigure the size and shape of said platform. A linear displacement mechanism moves the base of a non-redundant translational parallel manipulator vertically.

The robot shown in Fig. 2 comprises a reconfigurable fixed platform with a fixed element (6) and three mobile elements in the form of a framing square (7a, 7b, 7c). These framing squares simultaneously modify the radius and height between the axes of the motors (8a, 8b, 8c) and the center of the fixed element (6). In the center of the fixed platform, there is a screw (1) driven by a fourth actuator (8d). A nut (4) coupled to the screw slides along three guide bars (3a, 3b, 3c). The nut moves the framing squares according to the rotation and pitch of the screw (1) through coupling bars (5a, 5b, 5c). It is important to note that the set of components, i.e., screw (1), nut (4), motor (8d) and coupling bars (5a, 5b, 5c), establish a system used here only as a example of a linear displacement mechanism.
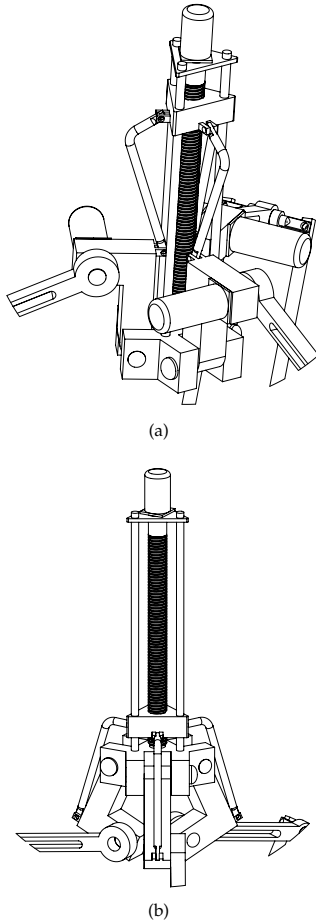

Figure 3. Vertical displacement position of the mobile elements. (a) Highest vertical displacement position. (b) Lowest vertical displacement position.

Fig. 3 shows the highest and lowest displacement of the mobile elements, generated by a fourth actuator. It should be noted that this configuration is highly versatile, since the

mechanism can also be reconfigured with decoupled motions for framing squares from the rest of the mechanism, enabling it to return to the original configuration and mechanical characteristics of the Parallix LKF-2040. Furthermore, by the redundancy effect customized solutions of the kinematic performance of the manipulator, can be obtained.
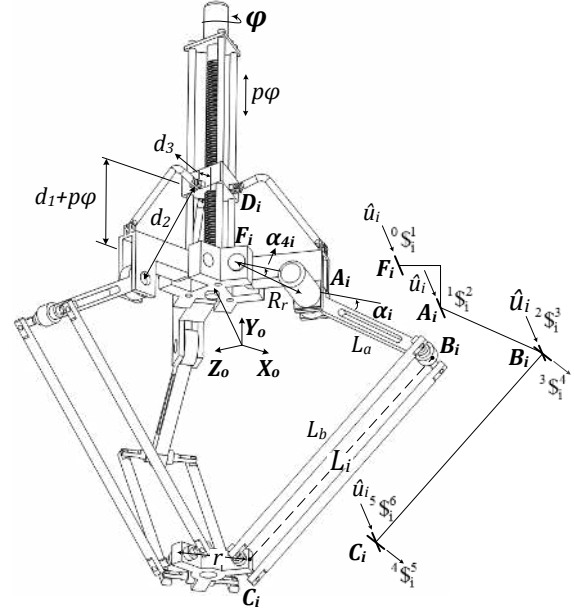

Figure 4. Geometrical parameters of the mechanism

Fig. 4 shows the geometrical parameters of the reconfigurable manipulator Parallix.

3. Kinematic Analysis of the Reconfigurable Manipulator

3.1 Position analysis

The forward position analysis consists of finding the location of the moving platform, given the generalized coordinates of the manipulator. This analysis is the equivalent of computing the coordinates of a point on the moving platform. In what follows, the forward position analysis is performed, based on the method introduced in [36, 37].

As an intermediate step, it is necessary to first calculate the generalized coordinate α_4. According to Fig. 4, it immediately emerges that:

$$\left(R_f + Rr\cos(\alpha_4) - d_3\right)^2 + \left(d_1 + p\varphi - Rr\sin(\alpha_4)\right)^2 = d_2^2$$

where d_1 is an offset between point D_i and the base plane of the nut, d_2 is the signed distance between points D_i and point A_i and d_3 is the perpendicular distance between the screw axis and point D_i. Meanwhile, p is the thread pitch of the screw. Then, solving the binomial, we have:

$$k_1 \sin(\alpha_4) + k_2 \cos(\alpha_4) = k_3 \qquad (1)$$

where

$$k_1 = -2Rr(d_1 + p\varphi)$$
$$k_2 = 2Rr(R_f - d_3)$$
$$k_3 = d_2^2 - R_f^2 - Rr^2 - d_3^2 + 2R_f d_3 - d_1^2 - p^2\varphi^2 - 2d_1 p\varphi$$

Following on, solving Eq. (1) for α_4, it follows that:

$$\sin(\alpha_4) = \frac{2k_1 k_3 \pm \sqrt{4k_1^2 k_3^2 - 4\left(k_1^2 + k_2^2\right)\left(k_3^2 - k_2^2\right)}}{2\left(k_1^2 + k_2^2\right)} \qquad (2)$$

Thus, with Eq. (2), the generalized coordinate α_4, generated by the linear displacement system and used as an example in this paper, is calculated.

Let $X_0 Y_0 Z_0$ be a reference frame whose origin is attached to the center of the fixed platform of the manipulator (see Fig. 4). The coordinates of the point $F_i = (Fx_i, Fy_i, Fz_i)$, located by the vector $\boldsymbol{F}_i$, as well as the coordinates of point $A_i = (Ax_i, Ay_i, Az_i)$, located by the vector $\boldsymbol{A}_i$, depends on the rotation φ of the motor. Therefore, $\alpha_{4i}(\varphi) = \alpha_4(\varphi)$, since α_{4i} is the same angle for all framing squares, while the coordinates of point $B_i = (Bx_i, By_i, Bz_i)$, located by the vector $\boldsymbol{B}_i$, are calculated by projections as follows:

$$F_1 = \begin{bmatrix} R_f & 0 & 0 \end{bmatrix}$$

$$F_{2,3} = \begin{bmatrix} R_f \sin(\theta_{2,3}) & 0 & R_f \cos(\theta_{2,3}) \end{bmatrix}$$

$$A_1 = \begin{bmatrix} Rr\cos(\alpha_4) + Fx_1 & Rr\sin(\alpha_4) + Fy_1 & 0 + Fz_1 \end{bmatrix}$$

$$A_{2,3} = \begin{bmatrix} Rr\cos(\alpha_4)\sin(\theta_{2,3}) & +Fx_{2,3} & Rr\sin(\alpha_4) + Fy_{2,3} \\ & & Rr\cos(\alpha_4)\cos(\theta_{2,3}) + Fz_{2,3} \end{bmatrix}$$

$$B_1 = \begin{bmatrix} La\cos(\alpha_1) + Ax_1 & By_1 & 0 + Az_1 \end{bmatrix}$$

$$B_{2,3} = \begin{bmatrix} La\cos(\alpha_{2,3})\sin(\theta_{2,3}) & +Ax_{2,3} & By_i \\ & & La\cos(\alpha_{2,3})\cos(\theta_{2,3}) + Az_{2,3} \end{bmatrix}$$

where $\theta_{2,3}$ is the orientation angle of kinematic chains 2 and 3, since kinematic chain 1 is coincident with the X_o-axis; R_f is the distance from the fixed reference system $X_o Y_o Z_o$ to

each point F_i. Evidently, $By_i = La\sin(\alpha_i) + Ay_i$ is equal for all kinematic chains of the mechanism. Unless otherwise, in the remaining contribution, $i = 1,2,3$.

In order to formulate the closure equations required to solve the displacement analysis of the robot, consider that the moving platform is an equilateral triangle $C_1 C_2 C_3$ of side r and center P, located by vector $\boldsymbol{P}$. Furthermore, consider that $C_1 = (X, Y, Z)$. Then, the coordinates of C_2 and C_3 can be formulated via the unknown coordinates X, Y and Z, representing point C_1 as follows:

$$C_2 = \left(X - r\sin(\pi/3), Y, Z - r\cos(\pi/3)\right)$$
$$C_3 = \left(X - r\sin(\pi/3), Y, Z + r\cos(\pi/3)\right) \qquad (3)$$

Following on, the three closure equations can be written as:

$$\left(\boldsymbol{C}_i - \boldsymbol{B}_i\right)\cdot\left(\boldsymbol{C}_i - \boldsymbol{B}_i\right) = Lb^2 \qquad (4)$$

that generate

$$X^2 + Y^2 + Z^2 + K_{i1}X + K_{i2}Y + K_{i3}Z + K_{i4} = 0 \qquad (5)$$

In this way, $K_{ij}(j=1,2,3,4)$ are obtained according to the parameters and generalized coordinates of the mechanism, e.g., $K_{11} = -2Bx_1$, $K_{12} = -2By_1$, $K_{13} = -2Bz_1$, $K_{14} = Bz_1^2 + By_1^2 + Bx_1^2 - Lb^2 \dots$, etc. Furthermore, following some computations on Eqs. (5), the unknowns X and Y can be expressed in terms of Z as follows:

$$X = W_1 Z + W_2, \quad Y = W_3 Z + W_4 \qquad (6)$$

where the coefficients $W_1, \dots, W_4$ are calculated according to the coefficients K_{ij}, e.g.,

$$W_1 = \frac{K_{33}\left(K_{22} - K_{12}\right) + K_{23}\left(K_{12} - K_{32}\right) + K_{13}\left(K_{32} - K_{22}\right)}{K_{21}\left(K_{32} - K_{12}\right) - K_{11}\left(K_{32} + K_{22}\right) - K_{31}\left(K_{22} + K_{12}\right)} \qquad (7)$$

Finally, substituting Eqs. (6) in any of Eqs. (5) produces a second-order equation in the unknown Z as follows:

$$aZ^2 + bZ + c = 0 \qquad (8)$$

where

$$a = 1 + W_1^2 + W_3^2$$
$$b = K_{11}W_1 + 2W_1 W_2 + K_{13} + 2W_3 W_4 + K_{12}W_3$$
$$c = K_{11}W_2 + W_4^2 + W_2^2 + K_{14} + K_{12}W_4$$

Eq. 8 indicates that the moving platform can reach two different poses. Finally, point P is calculated using Eq. (9) as follows:

$$P = \left(X - r\cos\left(\pi/3\right), Y, Z\right) \qquad (9)$$

Note that owing to the decoupled motion of the fourth generalized coordinate, the reconfiguration strategy does not complicate the forward position analysis as reported for the Delta-type robot when using this method.

The inverse position analysis is the computation of the generalized coordinates given the pose of the moving platform, i.e., when $P = (Px, Py, Pz)$ is known. Since the point $C_i = (Px + r\cos(\theta_i), Py, Pz + r\sin(\theta_i))$ is also known, the equation of a sphere centered at point B_i can be obtained as:

$$\left(Cx_i - Bx_i\right)^2 + \left(Cy_i - By_i\right)^2 + \left(Cz_i - Bz_i\right)^2 - Lb^2 = 0 \qquad (10)$$

Solving Eq. (10) produces:

$$
\begin{aligned}
&2La\left(Ay_i - Py\right)\sin\left(\alpha_i\right) + 2rPx\cos\left(\theta_i\right) - 2rAx_i\cos\left(\theta_i\right) - \\
&2rLa\cos\left(\alpha_i\right) - 2LaPz\cos\left(\alpha_i\right)\sin\left(\theta_i\right) + 2rPz\sin\left(\theta_i\right) - \\
&2rAz_i\sin\left(\theta_i\right) + 2LaAx_i\cos\left(\alpha_i\right)\cos\left(\theta_i\right) + \\
&2LaAz_i\cos\left(\alpha_i\right)\sin\left(\theta_i\right) - 2LaP_x\cos\left(\alpha_i\right)\cos\left(\theta_i\right) + Px^2 - \\
&2PxAx_i + Ax_i^2 + Py^2 - 2PyAy_i + Ay_i^2 + Pz^2 - 2PzAz_i + \\
&Az_i^2 + r^2 + La^2 - Lb^2 = 0
\end{aligned}
$$

Thus, a few algebraic steps later and by substituting for Q_i and S_i we have:

$$2(Ay_i - Py)\sin(\alpha_i) + Q_i\cos(\alpha_i) = S_i \qquad (11)$$

where

$$
\begin{aligned}
Q_i = -2r - 2Pz\sin\left(\theta_i\right) + \ &2Ax_i\cos\left(\theta_i\right) + \\
&2Az_i\sin\left(\theta_i\right) - 2Px\cos\left(\theta_i\right)
\end{aligned}
$$

$$
\begin{aligned}
S_i = &\frac{2r\left(\left(Ax_i - Px\right)\cos\left(\theta_i\right) + \left(Az_i - Pz\right)\sin\left(\theta_i\right)\right)}{La} + \\
&\frac{-Px^2 + 2PxAx_i - Ax_i^2 - Py^2 + 2PyAy_i -}{} \\
&\frac{Ay_i^2 - Pz^2 + 2PzAz_i - Az_i^2 - r^2 - La^2 + Lb^2}{La}
\end{aligned}
$$

With the aim to solve α_i from Eq. (11), the half-angle trigonometric identity is applied and simplification yields:

$$
-\left(Q_i + S_i\right)\left(\tan\left(\tfrac{\alpha_i}{2}\right)\right)^2 + 4\left(Ay_i - Py\right)\tan\left(\tfrac{\alpha_i}{2}\right) \quad -S_i
$$
$$
+Q_i = 0
$$

Finally, solving $\tan(\tfrac{\alpha_i}{2})$ generates:

$$\tan\left(\frac{\alpha_i}{2}\right) = \frac{-2Py + 2Ay_i \pm \sqrt{\begin{aligned}&4Py^2 \quad -8PyAy_i + 4Ay_i^2 \\ &+Q_i^2 - S_i^2\end{aligned}}}{Q_i + S_i} \qquad (12)$$

In Eq. (12), it is important to note that Ay_i is the coordinate reflecting redundancy as generated by the reconfiguration. However, Ay_i is only known for the inverse position analysis, since the redundancy problem is addressed in the following sections, which is solved based on optimization of a performance index.

3.2 Manipulator workspace

In order to show the shape of the workspace and obtain its approximate volume generated by the reconfiguration, the inverse position analysis is applied. Using Eq. (12) and defining discrete configurations for $90 \le \alpha_4 \le -90$ for each of the framing squares (it is evident that α_4 is the same angle for each one of them), the shape of the workspace generated by the reconfiguration is obtained by sweeping the three-dimensional space $SO(3)$ and discarding any non-real solutions. It should be noted that, when $\alpha_{4i} = 0°$, the workspace of the original configuration of the Parallix LKF-2040 is produced.

The dimensions (SI) considered for computing the robot workspace are: $La = 0.2$, $Lb = 0.4$, $r = 0.8660$, $R_f = 0.05$ and $Rr = 0.1118$, as shown in Fig. 5.(a). In Fig. 5.(b), this is $0 \le Rr \le 0.1618$, because of the reconfiguration effects.

The entire reconfigurable manipulator workspace is shown in Fig. 5.(b), where the union of workspaces for different configurations of the mechanism corresponds to a volume of $0.2359 m^3$. On the other hand, in Fig. 5.(a), the original workspace has a volume of $0.0698 m^3$. Both figures and their volumes were calculated using the computational software Geomagic.

Fig. 5.(b) shows that the geometrical shape of entire workspace is similar to a sphere, which is desirable in a parallel manipulator. Furthermore, the current workspace is a paraboloid with three concavities and with a smaller volume than the workspace generated by the reconfigurable manipulator. It is worth noting that the significant increase of the manipulator workspace is one of additional advantages obtained by the reconfiguration strategy effects.
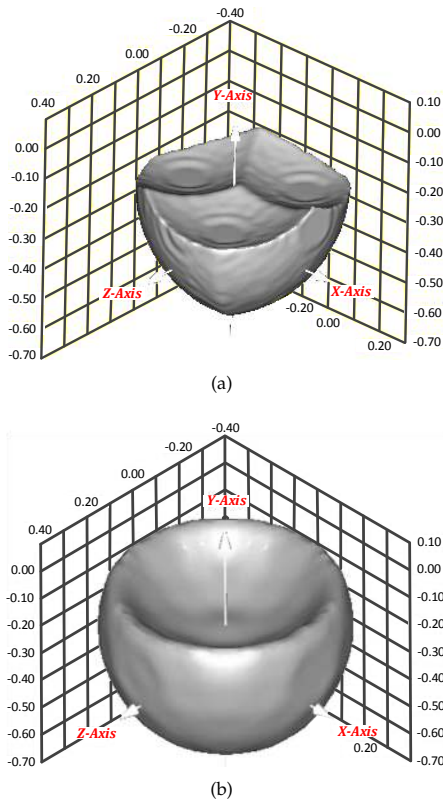
(a)

(b)

Figure 5. Workspace of reconfigurable parallel Parallix manipulator

3.3 Velocity analysis

Velocity analysis involves determining the velocity state of the moving platform with respect to the fixed platform [36, 37] when the joint rates are known as follows:

$$\dot{q}_4 = \frac{d}{dt}\alpha_4, \quad \dot{q}_i = \frac{d}{dt}\alpha_i$$

The joint rate $\dot{q}_4$ can be geometrically computed according to the linear displacement device installed in the manipulator (Fig. 4). Hence, in this work $\dot{q}_4$ is the derivative gained via Eq. (2) and will be used as an independent variable in the velocity analysis.

Let $V = [0, v]^T$ be the velocity state of the moving platform as observed from the fixed platform, where v is the velocity vector of any point on the moving platform. The velocity state V can be expressed in screw form through the limbs of the robot as follows:

$$\dot{q}_4 \, {}^0\$_i^1 + \dot{q}_i \, {}^1\$_i^2 +_2 \omega_3^i \, {}^2\$_i^3 +_3 \omega_4^i \, {}^3\$_i^4 +_4 \omega_5^i \, {}^4\$_i^5 + {}_5 \omega_6^i \, {}^5\$_i^6 = V \tag{13}$$

where i denotes the i-th kinematic chain. In order to obtain an input-output velocity equation for the reconfigurable manipulator, consider that

$L_i = [l x_i \quad l y_i \quad l z_i \quad L\, x_i \quad L\, y_i \quad L\, z_i]^T$ is a line in the Plücker coordinates that passes through the points B_i and C_i (Fig. 4) and is reciprocal to all the screws in the same limb, except for the screw associated with the actuated revolute joint. Therefore, the systematic application of the Klein form, which is denoted as $\{*\,;*\}$, of the line L_i to both sides of Eq. (13) can be expressed as follows:

$$\left\{\dot{q}_4 \, {}^0\$_i^1 + \dot{q}_i \, {}^1\$_i^2 +_2 \omega_3^i \, {}^2\$_i^3 + \ldots +_5 \omega_6^i \, {}^5\$_i^6 ; L_i\right\} = \left\{V; L_i\right\}$$

And reducing terms we have

$$\left\{{}^2\$_i^3 ; L_i\right\} = \left\{{}^3\$_i^4 ; L_i\right\} = \left\{{}^4\$_i^5 ; L_i\right\} = \left\{{}^5\$_i^6 ; L_i\right\} = 0$$

Accordingly, $\dot{q}_4\{{}^0\$_i^1 ; L_i\} + \dot{q}_i\{{}^1\$_i^2 ; L_i\} = \{V; L_i\}$ yields the input-output velocity equation as:

$$\mathbf{A}v = \mathbf{B}'\dot{\mathbf{q}}_4 + \mathbf{B}\dot{\mathbf{q}} \tag{14}$$

In this way,

$\mathbf{A} = [l x_i \quad l y_i \quad l z_i]^T$ is the active Jacobian matrix of the manipulator, while $\dot{\mathbf{q}}_4 = [\dot{q}_4 \quad \dot{q}_4 \quad \dot{q}_4]^T$ and $\dot{\mathbf{q}} = [\dot{q}_1 \quad \dot{q}_2 \quad \dot{q}_3]^T$ are the first-order generalized coordinates of the mechanism.

$\mathbf{B}' = diag\left[\{0\$_1^1 ; L_1\} \quad \{0\$_2^1 ; L_2\} \quad \{0\$_3^1 ; L_3\}\right]$ and

$\mathbf{B} = diag\left[\{1\$_1^2 ; L_1\} \quad \{1\$_2^2 ; L_2\} \quad \{1\$_3^2 ; L_3\}\right]$ are the passive Jacobian matrices.

3.4 Acceleration analysis

Reduced acceleration state analysis using screw theory for robot manipulators was introduced by [38].

Let $A = [0, a]^T$ be the acceleration state of the moving platform as observed from the fixed platform, where a is the acceleration vector of any point on the moving platform and can be expressed in screw form via the limbs of the robot as follows:

$$\ddot{q}_4 \, {}^0\$_i^1 + \ddot{q}_i \, {}^1\$_i^2 +_2 \dot{\omega}_3^i \, {}^2\$_i^3 +_3 \dot{\omega}_4^i \, {}^3\$_i^4 + {}_4 \dot{\omega}_5^i \, {}^4\$_i^5 +_5 \dot{\omega}_6^i \, {}^5\$_i^6 + \mathcal{L}_i = A \tag{15}$$

Where $\mathcal{L}_i$ is the screw of acceleration computed as:

$$\begin{aligned}\mathcal{L}_i = &\left[\dot{q}_4 \, {}^0\$_i^1 \quad \dot{q}_i \, {}^1\$_i^2 + \ldots +_4 \omega_5^i \, {}^4\$_i^5 +_5 \omega_6^i \, {}^5\$_i^6\right]\\ &+\left[\dot{q}_i \, {}^1\$_i^2 \quad {}_2\omega_3^i \, {}^2\$_i^3 +_3 \omega_4^i \, {}^3\$_i^4 +_4 \omega_5^i \, {}^4\$_i^5 +_5 \omega_6^i \, {}^5\$_i^6\right]\\ &+\left[{}_2\omega_3^i \, {}^2\$_i^3 \quad {}_3\omega_4^i \, {}^3\$_i^4 +_4 \omega_5^i \, {}^4\$_i^5 +_5 \omega_6^i \, {}^5\$_i^6\right]\\ &+\left[{}_3\omega_4^i \, {}^3\$_i^4 \quad {}_4\omega_5^i \, {}^4\$_i^5 +_5 \omega_6^i \, {}^5\$_i^6\right]\\ &+\left[{}_4\omega_5^i \, {}^4\$_i^5 \quad {}_5\omega_6^i \, {}^5\$_i^6\right]\end{aligned} \tag{16}$$

In this way, the brackets [* *] denote the Lie product of the Lie algebra $se(3)$ of the Euclidean group $SE(3)$. Hence, applying the Klein form analogously to velocity analysis we have:

$$\ddot{q}_4\left\{{}^0\$_i^1;L_i\right\} + \ddot{q}_i\left\{{}^1\$_i^2;L_i\right\} + \left\{\mathcal{L}_i;L_i\right\} = \left\{A;L_i\right\}$$

Therefore, the input-output equation of acceleration for the manipulator is:

$$\mathbf{A}a = \mathbf{B}'\ddot{\mathbf{q}}_4 + \mathbf{B}\ddot{\mathbf{q}} + \mathbf{C} \qquad (17)$$

where $\ddot{\mathbf{q}}_4 = [\ddot{q}_4 \quad \ddot{q}_4 \quad \ddot{q}_4]^T$ and $\ddot{\mathbf{q}} = [\ddot{q}_1 \quad \ddot{q}_2 \quad \ddot{q}_3]^T$ are the second-order generalized coordinates of the mechanism, while $\mathbf{C} = [\{\mathcal{L}_1;L_1\} \quad \{\mathcal{L}_2;L_2\} \quad \{\mathcal{L}_3;L_3\}]^T$ is the complementary matrix of acceleration.

3.5 Evident singular configurations

The singular configurations or singularities, according to [39, 40], can be deduced from Eq. (14). Such configurations are distinct for the fixed platform and the rest of the mechanism, since they are uncoupled mechanisms. However, when there exist combined singularities between these two mechanisms, the reconfigurable manipulator itself will be in a fully singular pose.

In this context, singularities of the Delta-type robot occurs when:

1. If $det(\mathbf{A})=0$, then the links Lb are collinear or parallels. In these configurations, the moving platform gains degrees of freedom.

2. If $det(\mathbf{B})=0$, then links La are completely folded or unfolded. In such configurations, the mobile platform loses degrees of freedom.

3. If $det(\mathbf{A})=0$ and $det(\mathbf{B})=0$, then the fixed platform and the moving platform are coplanar, e.g., when the moving platform has an identical geometry to that of the fixed platform and the limbs are vertical.

It should be noted that the singularity locus remains the same as for a Delta-type robot. This condition shows that the reconfiguration strategy does not drastically affect the structure of this parallel robot. It is also important to note that the Delta-type mechanism is capable of avoiding singularities by using the redundancy of the reconfigurable robot, which is an additional advantage of the proposed strategy in this paper.

On the other hand, the fixed platform, which is reconfigurable, has its own singular configurations that may occur when $det(\mathbf{B}')=0$, e.g., when the mobile elements are folded or unfolded.

4. Numerical Example

In this section, a numerical example is provided to show that by redundancy customized solutions of the kinematic

performance can be obtained. To do so, computation of the condition number is used as a performance index and according to prescribed trajectories.

Three Cartesian trajectories of the center P of the moving platform are generated by solving the forward position analysis by considering $\alpha_{1,3}(t)=0.25\sin(t)$ and $\alpha_2(t)=0.25\cos(t)$, where the interval for time t is selected as $0 \le t \le 2\pi$, with values defined as $\alpha_4=45$,0 ,-45 (see Fig. 6). The link lengths are the same as in subsection 3.2 and the direction of the rotation axes of the active joints are defined by $\hat{u}_1=-\hat{k}$, $\hat{u}_2=-0.866\hat{i}+0.5\hat{k}$ and $\hat{u}_3=0.866\hat{i}+0.5\hat{k}$.
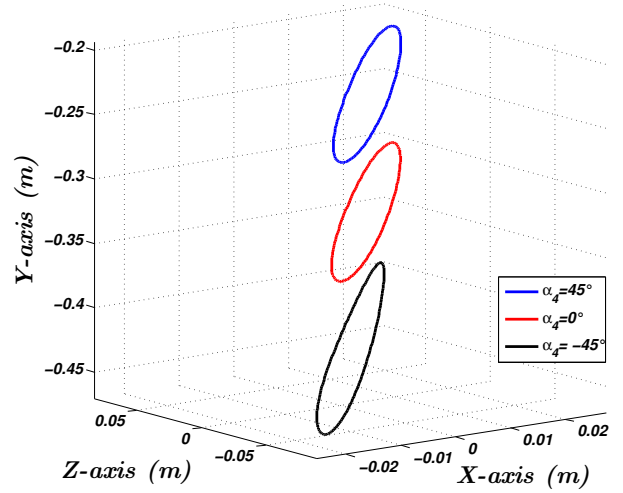

Figure 6. Trajectories of the center P at different angles of the reconfiguration coordinate α_4

In Fig. 6, the blue and red trajectories are very similar in size, because in the blue trajectory, the mobile elements reconfigure the fixed platform to a length close to that of the original configuration of the mechanism (red trajectory). On the other hand, the third trajectory (black color) has a large radius, because the length and height of the fixed platform is lower than for the other configurations, thereby producing greater angular movement in the actuated links.

The resulting temporal behaviour of the velocity and acceleration of the moving platform, associated with each trajectory shown in Fig. 6, is shown in Fig. 7 and Fig. 8, respectively.

It is evident that the velocity and acceleration components of the black circle (see Fig. 6) have greater amplitude than in the other two circles, since the length of the fixed platform is shorter than in the other two configurations. In other words, when $\alpha_4=-45°$, the reconfigurable robot carries out the black circle faster, meaning greater angular movement of actuated links.

4.1 Reconfiguration effects on the manipulator's performance

The Reference [41] defines the condition number as describing the accuracy/dexterity and the closeness to a
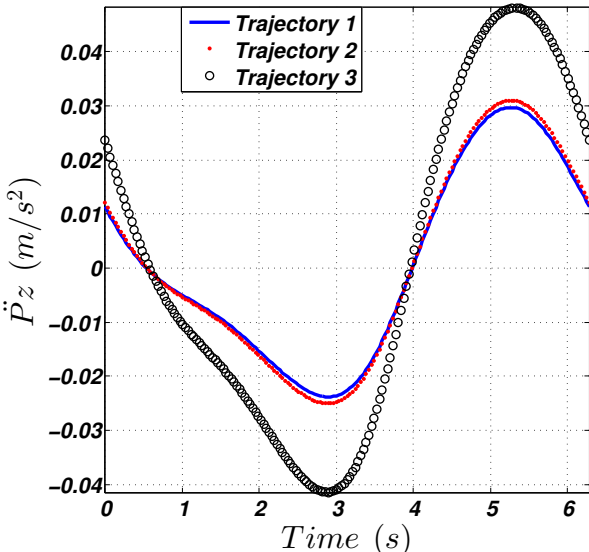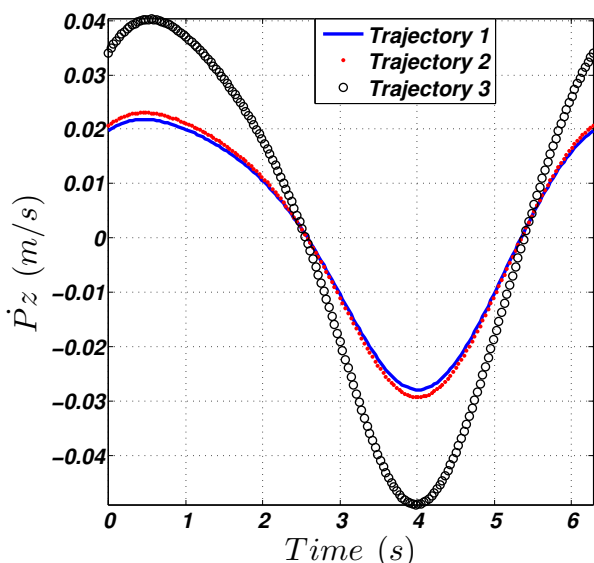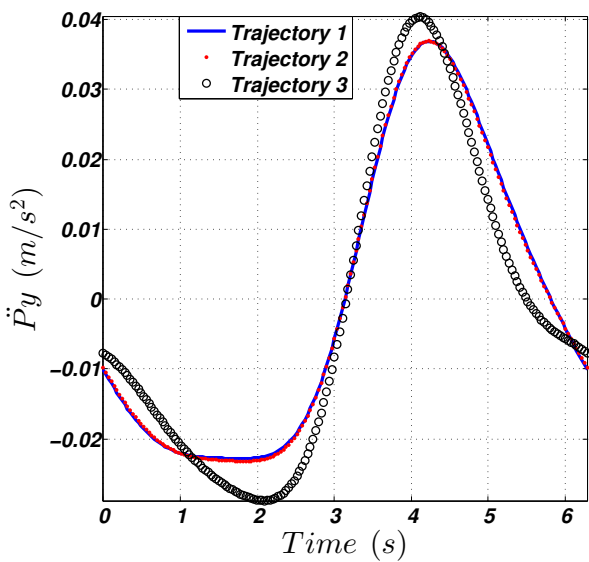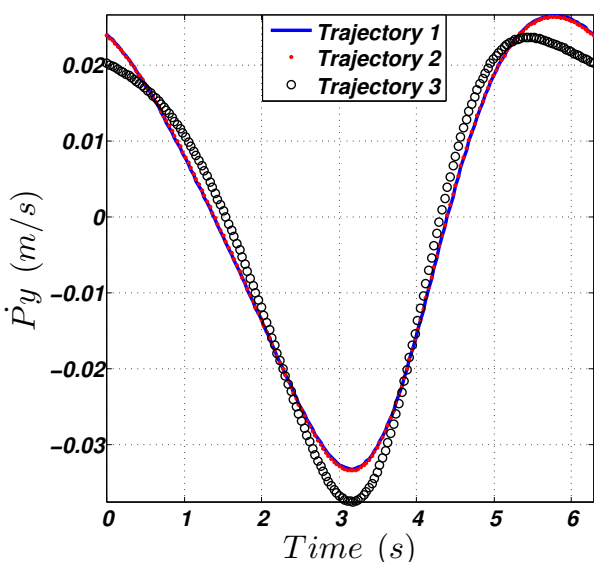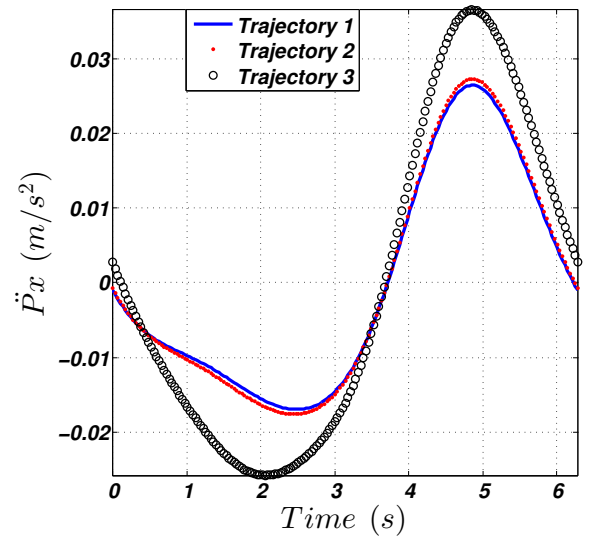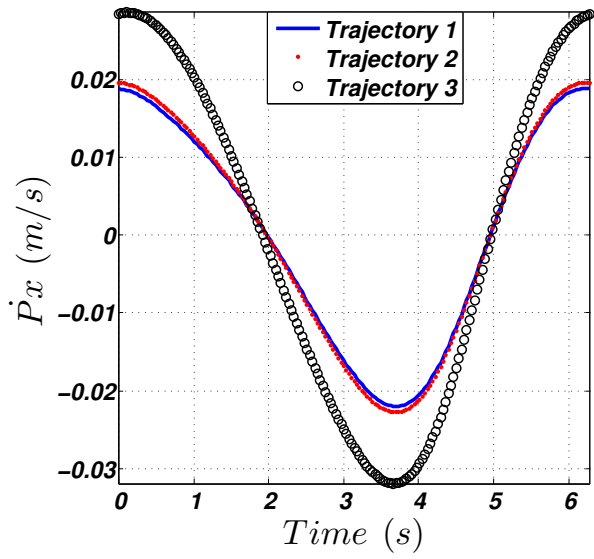
Figure 7. Velocity components of the center of the moving platform

Figure 8. Acceleration components for the center of the moving platform

singular configuration of a parallel manipulator. In the case of a Delta-type robot, the condition number has often been used as a performance index (see the aforementioned references) for evaluating its kinematic performance. In this subsection, the result of this performance index is improved by using the redundancy of the reconfiguration. The condition number is expressed as:

$$k = \left\| \mathbf{J}^{-1} \right\| \left\| \mathbf{J} \right\| \tag{18}$$

As a first step, it is necessary to calculate the Jacobian matrix $\mathbf{J}$ of the manipulator and then compute the condition number. The Jacobian matrix $\mathbf{J}$ is obtained from Eq. (14) as:

$$v = \left(\mathbf{A}^{-1} \mathbf{B} \right) \dot{\mathbf{q}} = \mathbf{J} \dot{\mathbf{q}} \tag{19}$$

We here use the matrix $\mathbf{J}$ of the well-known architecture of the Delta-type robot to demonstrate that it is possible to enhance its kinematic performance through redundancy of the proposed reconfiguration. Therefore, the first term of Eq. (14) depends on $\dot{q}_4$, as well as $k(\alpha_4)$, given that the best solution of k is computationally obtained by sweeping all possible combinations of α_4 in a range of $90° \leq \alpha_4 \leq -90°$ and seeking locally for each one of the trajectory points.

Noted that the inverse of the condition number k^{-1} is used, since it has a range between $0 \leq k^{-1} \leq 1$, where 0 indicates that the Jacobian matrix is not invertible and hence, the manipulator cannot generate velocities in some directions; this condition has been referred to as being a singular configuration [39]. When $k^{-1} = 1$, the manipulator is capable of generating velocities in any direction, in other words, to be in an isotropic pose [41].

The best values of k^{-1} are obtained for the 181 points of each trajectory by using the redundancy of the reconfiguration and they are compared with k^{-1} values, obtained with the original architecture of a Delta-type robot, namely with the Parallix robot (see Fig. 9)

In Fig. 9.(a) it can be seen that the performance of the proposed mechanism is better than for the Delta-type robot, despite the fact that such a mechanism is close to a singularity at specific trajectory points (e.g., points 43 and 101). In fact, the values of k^{-1} remain constant in the last 41 points of such a trajectory. On the other hand, the Parallix robot is not able to carry out the trajectory at intervals between 0 - 86 and 156 - 181; therefore, at these intervals, such a robot cannot reach the corresponding trajectory points.
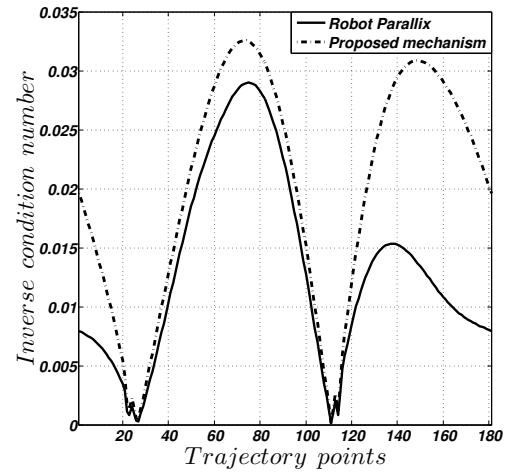
Figure 9.(b) shows that values obtained for the Delta-type robot are for the most part less than 0.01; however, by using redundancy, the performance of such a robot can be significantly increased, except in points 102 and 116, where the reconfigurable mechanism is close to a singular pose.
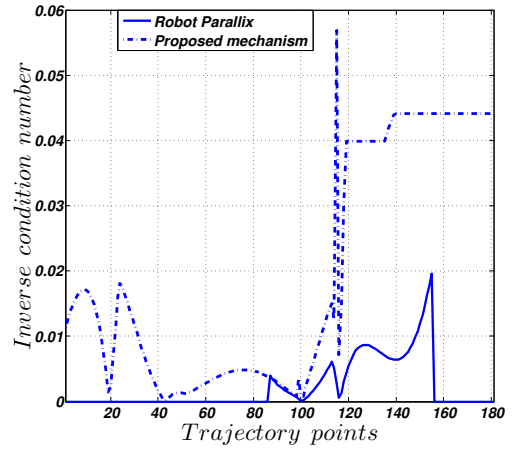
(a)
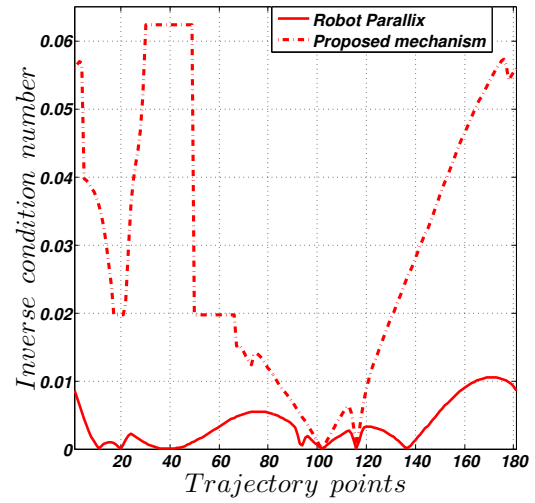
(b)

(c)

Figure 9. Value of k^{-1} for each trajectory of Fig. 6. (a) First circle (blue). (b) Second circle (red). (c) Third circle (black).

Nevertheless, it is worth noting that the reconfigurable robot is capable of avoiding many singularities, much more so than the original robot.

On the other hand, Fig. 9.(c) shows similar behaviour of the condition number for both robots, given that a part of this trajectory is performed within the boundaries of the manipulator workspace and therefore, the manipulators are close to a singularity in points 27 and 111. However, it is evident that an improvement in performance of the Delta-type robot has been obtained, primarily at the beginning and end of the trajectory.

It is important to note that by using redundancy, it is possible to achieve better performance in all the trajectories, compared to the performance achieved only with the Delta-type configuration, i.e., when $\alpha_4 = 0°$. Hence, as the condition number is improved in each trajectory by the reconfiguration, all other performance indices that dependent on matrix **J** of the manipulator, e.g., manipulability index, minimum singular value, global conditioning index, global manipulability index, etc., will also be improved.

5. Conclusions

In this paper, a reconfiguration strategy for a Delta-type parallel robot is proposed. The proposal is currently in the patenting process at IMPI - Mexico. The proposed reconfigurable manipulator is highly versatile, since it is able return to the original configuration and initial mechanical characteristics.

Customized solutions of the manipulator kinematic performance can be obtained by using redundancy generated by the reconfiguration. Additional advantages include an increased workspace and avoiding singularities.

The kinematic analysis was calculated by resorting to reciprocal-screw theory and evident singular configurations were analysed. It is worth noting that the manipulator did not change its singularity locus; this represents a significant advantage, since the original mechanism is not drastically affected by the reconfiguration strategy, thereby preserving mechanical simplicity.

Finally, a numerical example of the effects of the reconfiguration on the manipulator performance is presented. A calculation for the best condition number according to prescribed trajectories at different heights of the manipulator workspace was obtained. The results show that by using redundancy, the condition number is improved in each trajectory; accordingly, all performance indices that dependent on the Jacobian matrix are also improved.

6. References

[1] Krefft M, et al. A reconfigurable parallel robot with high flexibility. In: Proceeding of ISR Robotik 2006 - Joint Conference Robotics München.

[2] du Plessis L.J, Snymar J.A. An optimally re-configurable planar Gough-Stewart machining platform. Mechanism and Machine Theory 41 (2006), pp. 334-357.

[3] Kumar Satheesh G, Nagarajan T, Srinivasa Y.G. Characterization of reconfigurable Stewart platform for contour generation. Robotics and Computer-Integrated Manufacturing. 25 (2009), pp. 721-731.

[4] Zhiming J, Phillip S. Design of a reconfigurable platform manipulator. Journal of Robotic Systems 15(6), 1998, pp. 341-346.

[5] Gogu G. Isogliden-TaRb: a family of up to five axes reconfigurable and maximally regular parallel kinematic machines. Journal Manufacturing Systems, 36(5), 2007, pp. 419-426.

[6] Haage M, et al. Reconfigurable parallel Kinematic Manipulator for flexible manufacturing. 13th IFAC Symposium on Information Control Problems in Manufacturing, Vol 13, part 1, 2009, pp. 145-150.

[7] Brisan C, Csiszar A. Computation and analysis of the workspace of a reconfigurable parallel robotic system. Mechanism and Machine Theory 46 (2011), pp. 1647-1668.

[8] Xi F, Xu Y, Xiong G. Design and analysis of a reconfigurable parallel robot. Mechanism and Machine Theory. 41 (2006), pp. 191-211.

[9] Yang G, et al. Design and kinematic analysis of modular reconfigurable parallel robots. International Conference on Robotics and Automation, Proceedings 1999.

[10] Pisla D, et al. Kinematics and design of two variants of a reconfigurable parallel robot. Reconfigurable Mechanisms and Robots, 2009. ReMAR 2009. ASME/IFToMM International Conference on, pp. 624-631.

[11] Tosi D, et al. Cheope: A new reconfigurable redundant manipulator. Mechanism and Machine Theory 45 (2010), pp. 611-626.

[12] Bi Z.M, Wang L. Optimal design of reconfigurable parallel machining systems. Robotics and Computer-Integrated Manufacturing 25 (2009), pp. 951-961.

[13] Plitea N, et al. Structural design and kinematics of a new parallel reconfigurable robot. Robotics and Computer-Integrated Manufacturing 29 (2013), pp. 219-235.

[14] Carbonari L, et al. A new class of reconfigurable parallel kinematic machines. Mechanism and Machine Theory 79 (2014), pp. 173-183.

[15] Simaan N, Shoham M.. Stiffness synthesis of a variable geometry six-degrees-of-freedom double planar parallel robot. The International Journal of Robotics Research, 22(9), 2003, pp. 757-775.

[16] Borràs J, et al. A reconfigurable 5-DoF 5-SPU parallel platform, ASME/IFToMM International Conference on Reconfigurable Mechanisms and Robots, 2009, pp. 617-662.

[17] Zhang D, Shi Q. Novel design and analysis of a reconfigurable parallel manipulator using variable geometry approach. Practical Applications of

Intelligent Systems. Advances in Intelligent and Soft Computing 124 (2012), pp. 447-457.

[18] Ye W, et al. A new family of reconfigurable parallel mechanism with diamond kinematotropic chain. Mechanism and Machine Theory 74 (2014), pp. 1-9.

[19] Kock S, Schumacher W. A parallel x-y manipulator with actuation redundancy for high-speed and active-stiffness applications. Robotics and Automation, 1998. Proceedings. 1998 IEEE International Conference on (Volume: 3), pp. 2295-2300.

[20] Bi Z.M, Kang B. Enhancement of adaptability of parallel kinematic machines with an adjustable platform. Journal of Manufacturing Science and Engineering, 132(6), 2010.

[21] Moosavian A, Xi F.(J). Design and analysis of reconfigurable parallel robots with enhanced stiffness. Mechanism and Machine Theory 77 (2014), pp. 92-110.

[22] Jiang Y, Li T-m, Wang L-p. Dynamic modeling and redundant force optimization of a 2-DOF parallel kinematic machine with kinematic redundancy. Robotics and Computer-Integrated Manufacturing 32 (2015), pp. 1-10.

[23] Li C, Zhang X.G, Zhao Y.S. Redundant actuation investigation of a 5-DOF parallel robot. Applied Mechanics and Materials 526, 2014, pp. 164-170.

[24] Kotlarski J, Heimann B, Ortmaier T. Improving the pose accuracy of planar robot using mechanism of variable geometry. Advances in Robot Manipulators, InTech, 2010.

[25] Kotlarski J, Heimann B, Ortmaier T. Influence of kinematic redundancy on the singularity-free workspace of parallel kinematics machines. Frontiers of Mechanical Engineering, 7(2), 2012, pp. 120-134.

[26] Cha S-H, Lasky T.A, Velinsky S.A. Singularity avoidance for the 3-RRR mechanism using kinematic redundancy. IEEE International Conference on Robotics and Automation, 2007, pp. 10-14.

[27] Xu B, et al. Workspace Analysis of the 4RRR Planar Parallel Manipulator with Actuation Redundancy. Tsinghu Science and Technology, 15(5), 2010, pp. 509-516.

[28] Yue S, Tso S.K, Xu W.L. Maximum-dynamic-payload trajectory for flexible robot manipulators with kinematic redundancy. Mechanism and Machine Theory 36 (2001), pp. 785-800.

[29] Chen C.-T. Reconfiguration of a parallel kinematic manipulator for the maximum dynamic load-carrying capacity. Mechanism and Machine Theory 54 (2012), pp. 62-75.

[30] Dan W, Rui F, Wuyi C. Performance enhancement of a three-degree-of-freedom parallel tool head via actuation redundancy. Mechanism and Machine Theory 71 (2014), pp. 142-162.

[31] Finistuari A.D, Xi F.(J). Reconfiguration analysis of a fully reconfigurable parallel robot. Journal of Mechanism and Robotics, 5(4), 2013.

[32] Jiang Y, Li T, Wang L. The dynamic modeling, redundant-force optimization, and dynamic performance analyses of a parallel kinematic machine with actuation redundancy. Robotica, 33, 2015, pp. 241-263.

[33] Wu J, Wang J, Wang L. Optimal kinematic design and application of a redundantly actuated 3DOF planar parallel manipulator. Journal of Mechanical Design, 130(5), 2008.

[34] Gonzalez-Hernandez A, Castillo-Castaneda E. Stiffness estimation of a parallel manipulator using image analysis and camera calibration techniques. Robotica, Vol. 31, 2013, pp. 657-667.

[35] Balmaceda A, Castillo E. Metodología de rediseño de un robot paralelo tipo Delta de 3-GDL en función de un espacio de trabajo prescrito. (In Spanish). Nexo, Revista Científica, 26(01), 2013, pp. 24-33.

[36] Gallardo J, Orozco H, Rico J.M. Kinematics of 3-RPS parallel manipulators by means of screw theory. International Journal of Advanced Manufacturing Technology, 36(5/6): pp. 598-605, 2008.

[37] Gallardo-Alvarado J, Balmaceda-Santamaría A.L, Castillo-Castaneda E. An application of screw theory to the kinematic analysis of a Delta-type robot. Journal of Mechanical Science and Technology, 28(9), 2014, pp. 3785-3792.

[38] Rico J.M, Duffy J. An application of screw algebra to the acceleration analysis of serial chains, Mechanism and Machine theory, 31(5), 1996, pp. 445-457.

[39] Tsai L.W. Robot analysis: The mechanics of serial and parallel manipulators. A Wiley-interscience publication, United States of America, 1999.

[40] Gosselin C, Angeles J. Singularity Analysis of closed-loop kinematic chains. IEEE, Transactions on Robotics and Automation, 6(3), 1990, pp. 281-290.

[41] Merlet J.P. Jacobian, manipulability, condition number and accuracy of parallel robots. Robotics Research. Springer Tracts in Advanced robotics, 8, 2007, pp. 175-184.